https://doi.org/10.1016/j.energy.2016.11.081

An optofluidic planar microreactor for photocatalytic reduction of CO_2 in alkaline environment

Xiao Cheng[a,b], Rong Chen[a,b]*, Xun Zhu[a,b]*, Qiang Liao[a,b], Liang An[c], Dingding Ye[a,b], Xuefeng He[a,b], Shuzhe Li[a,b], Lin Li[a,b]

[a] Key Laboratory of Low-grade Energy Utilization Technologies and Systems (Chongqing University), Ministry of Education, Chongqing 400030, China

[b] Institute of Engineering Thermophysics, Chongqing University, Chongqing 400030, China

[c] Department of Mechanical Engineering, The Hong Kong Polytechnic University, Hung Hom, Kowloon, Hong Kong, China

*Corresponding author:

[a,b] Tel.: 0086-23-65103119; fax: 0086-23-65102474; e-mail: rchen@cqu.edu.cn (Rong Chen)

[a,b] Tel.: 0086-23-65102474; fax: 0086-23-65102474; e-mail: zhuxun@cqu.edu.cn (Xun Zhu)

Abstract

The development of highly efficient photocatalytic reactor is of importance to improve the performance of the photocatalytic reduction of CO_2. In this work, an optofluidic planar microreactor is designed and fabricated for the photocatalytic reduction of CO_2 with liquid water in alkaline environment. Such design offers several advantages of large surface-area-to-volume ratio, enhanced mass and photon transfer and more uniform light distribution. The performance of the developed planar microreactor is evaluated by measuring the methanol concentration to estimate the methanol yield under various operating parameters, including the liquid flow rate, light intensity, catalyst loading and NaOH concentration. It is shown that increasing the liquid flow rate firstly improves and then decreases the methanol concentration while the methanol yield continuously increases as the liquid flow rate increases. The

increase of the light intensity and NaOH concentration increases both the methanol concentration and yield. Increasing the catalyst loading firstly improves the performance and then results in the reduction of the performance. A maximum methanol yield of 454.6 μmole/g-cat·h is achieved under a liquid flow rate of 50 μL/min, 0.2 M NaOH, and the light intensity of 8 mW/cm^2.

Keywords: Optofluidic planar microreactor; photocatalytic reduction of CO_2; methanol concentration; methanol yield

1. Introduction

Rapid depletion of fossil fuels not only causes the problem of national energy security but also generates a great amount of CO_2, which is a primary greenhouse gas and main contribution to global warming. It is estimated that the atmospheric CO_2 concentration has increased more than 39% from the pre-industrial, leading to the global temperature increase of about 0.8°C [1, 2]. According to the Intergovernmental Panel on Climate Change (IPCC) 5th Assessment Report (AR5), the global temperature increasing is critically associated with the increase of greenhouse gas emission [3]. For this reason, extensive efforts have been paid to reduce CO_2 emission [4-9]. Among them, carbon capture and storage (CCS) is the most popular technology for capturing CO_2 but it usually requires an additional fuel input of 25 to 80 % and takes several steps in the whole process including separation, purification, compression, transportation and storage [10]. A promising way with increasing

attention is the reduction of CO_2 by photocatalysis, which not only captures CO_2 but also simultaneously generates solar fuels. In the CO_2 photoreduction technology, the abundant and low-cost raw materials are usually required, such as semiconductors or transition-metal complexes. Besides, no additional energy input is required except for the solar irradiation. Moreover, the photocatalytic reaction can take place under mild conditions. Therefore, the photocatalytic reduction of CO_2 possesses the economical and environmentally-friendly character in the CO_2 capture [11-13].

At present, in terms of the state of supplied water, the CO_2 photoreduction can be divided into two types: vapor-fed water and liquid-fed water. For the latter, the reactants are usually CO_2-saturated deionized water or CO_2-bubbled alkaline (like NaOH, $NaCO_3$, $NaHCO_3$) solution [14], because OH- ions are good holes scavengers. For the CO_2 photoreduction in liquid-fed water, various organic products can be obtained, including CH_4, CH_3OH, HCHO, HCOOH [15-17]. Taking CH_3OH as a product example, the reactions of the photocatalytic reduction of CO_2 to methanol in the alkaline environment can be described as follows [18],

$$TiO_2 + h\nu \rightarrow h^+ + e^- \quad (1)$$

$$H_2O + h^+ \rightarrow \cdot OH + H^+ \quad (2)$$

$$\cdot OH + H_2O + 3h^+ \rightarrow O_2 + 3H^+ \quad (3)$$

$$CO_2 + 6H^+ + 6e^- \rightarrow CH_3OH + H_2O \quad (4)$$

$$CO_3^{2-} + 8H^+ + 6e^- \rightarrow CH_3OH + 2H_2O \quad (5)$$

The electron-hole pairs are generated upon illumination. At the valance band, the

holes react with water to generate oxygen and protons, as indicated by Eqs. (1-3). If CO_2 is in the form of the molecules, CO_2 reacts with protons and photo-generated electrons to produce methanol and water (see Eq. (4)). When it is in the form of CO_3^{2-}, carbonate ions in the solution react with protons and photo-initiated electrons to produce methanol through a multi-electron transfer process (see Eq. (5)). By this way, CO_2 can then be converted into solar fuels via the photocatalytic reduction. However, current yields of solar fuels are still rather poor. One of the limitations comes from the vast majority of photocatalysts that do not exhibit good photoresponse to visible light [12]. Hence, much attempt has been made to the development of highly active photocatalysts with visible light response [19-22], like TiO_2 based catalysts [23, 24], $MnCo_2O_4$ [25], Bi_2WO_6 [26], $NiO/InTaO_4$ [27].

In addition to the photocatalysts, another limiting factor is the photoreactor design, which affects the mass transfer of CO_2, the light distribution and the specific surface area and thereby the performance of the photocatalytic CO_2 reduction. Main existing photoreactors for the CO_2 photoreduction have been summarized by Tahir and Amin [28], Das and Daud [11], Ola and Maroto-Valer [29], including slurry reactors, optical fiber reactors, monolith reactors, etc. Slurry reactors are the most common photoreactors, but suffer from the mass transfer resistance at the gas/liquid interface, non-uniform light distribution. Besides, the separation of catalysts also limits its efficiency and economy. Although these drawbacks can be overcome in optical fiber reactors, the fragility of the optical fibers and the durability of the catalysts on the

optical fiber still exist. In addition, optical fiber reactors have the problems of comparatively low surface area and low reactor volume for the photocatalysis process [30]. Monolith reactors containing parallel straight channels are considered to be more efficient for photocatalytic applications due to its high specific surface area, low pressure drop, ease in scale-up, etc. Nevertheless, due to the opacity of the honeycomb substrate, the light cannot efficiently penetrate through the channels so that the length of the monolith reactor is limited. Even though Liou *et al.* [31] developed the optical fiber monolith photoreactor to strengthen the light utilization, the light was still guided only by the optical fiber inserted into the apertures such that the monolith channels should be designed bigger, leading to inefficient distribution over the catalyst surface. In summary, the most existing photoreactors for the CO_2 photoreduction still suffer from the issues of low specific surface area, non-uniform light distribution and poor photon transfer.

Recently, a new interdisciplinary area of optofluidics that is synergy of microfluidics and optics has emerged. Such combination provides the advantages of fine flow control, large surface-area-to-volume ratio and enhanced mass transfer [32]. Besides, high spatial illumination homogeneity and better light penetration are also ensured. On the other hand, the photoreactors share the same feature with optofluidics, in which the fluids, light and their interaction are also included. In this case, the incorporation of optofluidics into the photoreactor design can greatly reduce the requirements for time, sample volume and equipment. Therefore, optofluidics has

become an ideal platform for the photocatalytic reaction systems. In a recent review by Wang *et al.* [32], it has been summarized that existing microreactors can be divided into several types, including micro-capillary, single-microchannel, multi-microchannel and planar microreactors. For the former three types of microreactors, the cross-section areas are usually small, limiting the throughputs. Moreover, the photon receiving areas are also small, leading to the inefficient utilization of the external irradiation light. However, for the planar microreactors, the photon receiving area is large. These characters show significant benefits for the photocatalytic system in many aspects including the throughput, the photon utilization, the fabrication of photocatalysts and the scalability to large-scale reactors. Because of these merits, the optofluidic planar microreactor has been adopted by various photocatalytic processes such as water splitting [33], water purification [34] and photocatalytic fuel cell [35]. Besides, Tahir *et al.* [30, 36] employed the microchannel monolith photoreactor for the CO_2-photoreduction with gaseous phase reactants and high performances were achieved. More recently, an optofluidic membrane microreactor has been developed for the photocatalytic reduction of CO_2 and also shown satisfactory performances [37]. However, although the superiority of the planar microreactor has been demonstrated, there is no open literature for the optofluidic planar microreactor towards the photocatalytic reduction of CO_2 with liquid water. Therefore, the objective of this study is to develop an optofluidic planar microreactor for the photocatalytic CO_2 reduction with liquid water in an alkaline environment. The feasibility and superiority of the developed optofluidic planar microreactor were

then assessed by measuring the methanol concentration at the outlet to estimate the methanol yield under different operating conditions, including the liquid flow rate, light intensity, catalyst loading and NaOH concentration.

2. Materials and methods

2.1 Design and fabrication of optofluidic planar microreactor

In this work, an optofluidic planar microreactor was designed, as sketched in Fig. 1a. The microreactor was comprised of one transparent rectangular reaction chamber as the top cover and the porous TiO_2 film coated glass as the bottom substrate. The porous TiO_2 film with 2 cm$\times$1 cm=2 cm^2 was located in the center of the reaction chamber with the dimension of 3 cm$\times$1.5 cm. The area of the reaction chamber was much bigger than that of the TiO_2 film, which ensured that the TiO_2 film was fully covered by the reaction chamber. Two syringe needles were connected to the inlet and outlet for the reactants supply and product collection. The tree-branch shaped microchannels at the inlet/outlet were adopted to ensure a uniform filling.

The reaction chamber was made by poly-(dimethysiloxane) (PDMS) since it was highly transparent. The fabrication process of the reaction chamber included two steps. The first step was the master mold processing by standard UV lithography [38]. A negative photoresist (SU-8, MicroChem) was spin-coated onto a silicon wafer cleaned by plasma cleaner (Mycro, HPC) and prebaked at 70, 80 and 90 ^oC with 10 minutes, respectively. The silicon wafer with the SU-8 photoresist was then exposed to 365 nm

UV light through a printed mask with the desired patterns. After the soft-bake at respective 70, 80 and 90 ^{o}C with 10 minutes, the unexposed photoresist was removed with a developer solvent to form the desired master mold and then post baked for 30 minutes. The second step was the PDMS chamber moulding. To do this, PDMS polymer base (Sylgard184, Dow Corning) and curing agent were mixed at a ratio of 10:1 and degassed. Then, the mixture was poured onto the patterned silicon wafer and baked at 95 °C for 0.5 h. After that, PDMS was uncovered from the patterned wafer substrate and cut by a knife into a reaction chamber chip. Finally, the developed PDMS chamber was bonded to a glass slide coated with the porous TiO_2 film to form an optofluidic planar microreactor, as shown in Fig. 1b.

2.2 Preparation of the porous TiO_2 film

The porous TiO_2 film on the glass slide was formed by the wet spray method. Before the spraying, the TiO_2 colloid was prepared by the sol-gel method [39]. First of all, 12 g TiO_2 (Degussa P25) powders, 120 mL distilled water and 0.4 mL acetylacetone (Sigma-Aldrich, USA) were mixed together with magnetic stirring. 0.2 mL Triton X-100 (Sigma-Aldrich, USA) and 2.4 g polyethylene glycol (Chengdu Kelong, China) were then added into the solution followed by continuous stirring for 12 h to form the TiO_2 colloid. With the prepared TiO_2 colloid, the wet spray could then be done. First, the glass slide cleaned by standard clean process was covered by a paper mask with a 2 cm$\times$1 cm hole. The prepared colloid was then sprayed onto the exposed region of the glass slide. After removing the mask, the TiO_2 coated glass was dried at room

183 temperature and then calcined in air at 550 °C for 2 h. A porous TiO_2 film with the
184 active surface area of 2 cm×1 cm=2 cm^2 coated onto the glass slide was formed. The
185 catalyst loading was determined by the weight difference between the mass of the
186 glass slide before spraying and the mass of catalyst coated glass slide after
187 calcinations over by the active surface area of 2 cm^2. Because some ingredients like
188 acetylacetone, polyethylene glycol in the TiO_2 colloid can be decomposed or
189 volatilized during the calcination, a little more TiO_2 colloid than the desired loading
190 was usually sprayed. As such, the final catalyst loading on the glass slide after
191 calcination could approach the desired value with small error. Moreover, several
192 catalyst coated glass slides for each catalyst loading were prepared. Only those
193 catalyst coated glass slides with the desired loading, i.e., the errors smaller than 0.1
194 mg/cm^2, were used to fabricate the optofluidic planar microreactors for the
195 performance evaluation. Fig. 2 depicts the microstructure of the porous TiO_2 film by
196 the field-emission scanning electron microscope (FE-SEM, Hitachi S4800). It can be
197 observed that the TiO_2 film had good porous microstructure, which provided
198 sufficient path for the transport of reactants and photons.
199
200 **2.3 Experimental setup**
201 The experimental system for the photocatalytic reduction of CO_2 with liquid water is
202 illustrated in Fig. 3. The microreactor was irradiated by a 100 W LED (Lightwells,
203 Shenzhen, China) at the wavelength of 365 nm with the light intensity controlled by
204 adjusting the distance between the microreactor and LED. In this work, the UV light

intensity was measured by a UV radiometer (UV-A, Photoelectric Instrument Factory of Beijing Normal University, China). During the operation, 99.99% CO_2 was continuously supplied to NaOH solution for 1 h to remove dissolved oxygen and saturate with CO_2. The addition of NaOH to create the alkaline environment is because OH^- ions are strong hole-scavengers that can hinder recombination of electron-hole pair. On the other hand, more CO_2 could be dissolved in the solution [40]. CO_2-saturated aqueous solution was then pumped into the microreactor by a syringe pump (Pump 33, Harvard). The products at the outlet were then collected for the analysis. It should be pointed out that in the process of the photocatalytic reduction of CO_2, several kinds of organics can be produced, such as methane, methanol, formic acid, and formaldehyde. Methanol is one of the basic and main products, which can be used as the fuel for direct methanol fuel cells [41]. In this work, hence, only the methanol concentration was analyzed by a GC (GC-2010 plus, Shimazu) equipped with FID detector using a 30-m Wax capillary column. To determine the methanol concentration, we purchased the chromatographic grade methanol (Aladdin, China) to prepare the standard CH_3OH solutions (5.0 mmol/L，1.0 mmol/L，0.8 mmol/L，0.4 mmol/L，0.2 mmol/L，0.1 mmol/L) for calibration. The chromatographic peak corresponding to methanol for a typical case could be read from the GC outputs (see Fig. 4), based on which the calibration curve for determining the methanol concentration could be obtained and the methanol peak in the real sample testing could be judged. With the measured methanol concentration, the methanol yield could be calculated to evaluate the performance of the

microreactor. Blank tests were conducted and no methanol was detected. All experiments were repeated at least three times at room temperature of about 25 ^{o}C.

3. Results and discussion

For such a photocatalytic system, the performance of the developed microreactor for the photocatalytic reduction of CO_2 is influenced by the operating and design parameters. Therefore, to access the performance of the developed microreactor, the effects of the liquid flow rate, light intensity, catalyst loading and NaOH concentration on the methanol yield were performed. Detailed results are presented in the following subsections.

3.1 Effect of the liquid flow rate

Figure 5 shows the variations of the methanol concentration and methanol yield with the liquid flow rate. In this work, the light intensity was maintained at 8 mW/cm^2, NaOH concentration was 0.2 M and the catalyst loading was about 2.5 mg/cm^2, while the liquid flow rate ranged from 12.5 μL/min to 100 μL/min. It is found that the methanol concentration at the outlet firstly increased and then decreased with the increase of the liquid flow rate. As known, when the liquid flow rate was rather low, although a large residence time could be achieved, which benefited for CO_2 to be involved in the photocatalytic reaction, less CO_2 and OH^- were supplied into the microreactor at the same time. Under such a circumstance, the inefficient supply of CO_2 may lead to the lowered methanol concentration. Meanwhile, less supply of OH^-

caused less holes to be captured, which also slowed down the photocatalytic reaction rate. On the other hand, too low liquid flow rate resulted in the generated methanol not to be efficiently washed away. As a result, the re-oxidation of methanol may take place [15], lowering the methanol concentration. However, as the liquid flow rate increased, the above mentioned problems could be overcome. Moreover, the increased liquid flow rate can not only greatly enhance the mass transport of CO_2 and OH^- to the catalyst layer to take part in the photocatalytic reaction but also benefit for the products removal to avoid the methanol re-oxidation. Therefore, the methanol concentration at the outlet increased as the liquid flow rate increased. However, once the liquid flow rate was too high, despite more reactants could be supplied and products could be more efficiently removed due to the enhanced mass transport, the residence time was greatly reduced, leading to less time for CO_2 in contact with the photocatalysts. Moreover, the generated methanol was also easily diluted. Therefore, the methanol concentration decreased with further increasing liquid flow rate. In this case, there existed an optimal liquid flow rate yielding maximal methanol concentration. According to the measured methanol concentrations under different liquid flow rates, the methanol yield M (μmole/g-cat·h), i.e., the amount of generated methanol per the catalyst mass and operation time, can be estimated by the following equation,

$$M = \frac{c \times 10^3 \times f \times 10^{-6} \times 60}{m \times 10^3} = \frac{c \times f \times 10^{-6} \times 60}{m} \quad (6)$$

where c (mmol/L) is the methanol concentration, f (μL/min) is the liquid flow rate and m (mg) is the total amount of the catalyst determined by the catalyst loading

271 (mg/cm^2) and active surface area (cm^2).

272

273 As shown in Fig. 4, unlike the variation of the methanol concentration with the liquid
274 flow rate, the methanol yield was always increased with the increase of the liquid
275 flow rate in the testing range. A maximum methanol yield of 289.3 μmole/g-cat·h was
276 obtained at a liquid flow rate of 100 μL/min. When the liquid flow rate was increased
277 from 12.5 μL/min to 25 μL/min, the methanol concentration was increased. The
278 reason can be referred to Eq. (6). The increase of the methanol concentration and
279 liquid flow rate could lead to an increase in the methanol yield. However, when the
280 liquid flow rate was further increased, although the methanol concentration decreased,
281 the liquid flow rate was increased. Since the variation of the liquid flow rate was more
282 significant than that of the methanol concentration, the methanol yield was still
283 increased with the liquid flow rate. The above results indicate that although there
284 existed a liquid flow rate leading to the maximum methanol concentration and the
285 methanol yield always increased with the liquid flow rate in the testing range.

286

287 **3.2 Effect of the light intensity**

288 The photocatalytic reduction of CO_2 is excited by incident light so that the light
289 intensity plays an important role in the methanol generation. Therefore, the effect of
290 the light intensity on the performance of the developed optofluidic planar
291 microreactor was also explored. In this testing, the flow rate of was maintained at 50
292 μL/min. NaOH concentration was 0.2 M and the catalyst loading was about 2.5

293 mg/cm^2. The light intensity ranged from 2 mW/cm^2 to 8 mW/cm^2. It should be noted
294 that the UV LED lamp used in this study was a cold light source so that the
295 temperature of the microreactor almost remained unchanged in all cases. In this
296 situation, the temperature effect can be neglected in this work. As shown in Fig. 6,
297 increasing the light intensity led to an increase in both the methanol concentration and
298 methanol yield. It is easy to understand that the increased light intensity can generate
299 more electron-hole pairs for the photocatalytic CO_2 reduction reactions. Therefore,
300 increasing the light intensity improved the methanol concentration and methanol yield
301 simultaneously.
302
303 **3.3 Effect of the NaOH concentration**
304 As known, the NaOH concentration influences not only the dissolved amount of CO_2
305 but also the utilization of the photo-initiated holes because OH^- is a strong
306 hole-scavenger. Hence, the effect of the NaOH concentration was investigated in this
307 work. Here, the NaOH concentration ranged from 0.05 M, 0.1 M, 0.2 M to 0.4 M. The
308 liquid flow rate was maintained at 50 μL/min, the light intensity was 8 mW/cm^2 and
309 the catalyst loading was about 2.5 mg/cm^2. The experimental results are shown in Fig.
310 7. It is seen that in the testing range, both the methanol concentration and yield
311 linearly increased with increasing the NaOH concentration. This is because the more
312 OH^- ions existed, the more holes could be scavenged to form hydroxyl radicals to
313 reduce the recombination of hole-electron pairs. On the other hand, higher NaOH
314 concentration allowed more CO_2 to be dissolved in the solution. In this case, more

315 CO_2 can be photo-reduced to generate methanol. As a consequence, both the
316 methanol concentration and yield increased with the NaOH concentration.
317
318 **3.4 Effect of the catalyst loading**
319 Because the catalytic layer thickness that depends on the catalyst loading can affect
320 not only transport of CO_2, OH^- and photon inside this layer but also the active surface
321 area for the photocatalytic reaction of CO_2, the effect of the catalyst loading on the
322 CO_2 photoreduction performance was also studied. To do this, the catalyst loadings
323 were about 0.6 mg/cm^2, 1.7 mg/cm^2, 2.5 mg/cm^2, 3.5 mg/cm^2 with the errors smaller
324 than 0.1 mg/cm^2. The liquid flow rate was 50 μL/min, while the light intensity and
325 NaOH concentration were 8 mW/cm^2 and 0.2 M, respectively. Fig. 8 shows the
326 variations of the methanol concentration and yield with the catalyst loading. As seen,
327 both the methanol concentration and yield increased when the catalyst loading was
328 increased from 0.6 mg/cm^2 to 1.7 mg/cm^2. The reason is that when the catalyst
329 loading was too low, the thickness of the catalytic layer was also rather small.
330 Although the transport resistances of the CO_2, OH^- and photon in association with the
331 catalytic layer were reduced, the active surface area was small and less electron-hole
332 pairs were generated because of low catalyst loading. In this case, the photocatalytic
333 reaction rate became small, resulting in low methanol concentration and yield.
334 Increasing the catalyst loading led to the increase of the active surface area and
335 generated electron-hole pairs. Although the mass transfer resistances were increased,
336 the contribution of the above positive effects was more significant. Consequently, the

methanol concentration and yield simultaneously improved with increasing the catalyst loading. However, when the catalyst loading was further increased from 1.7 mg/cm^2 to 3.5 mg/cm^2, both the methanol concentration and yield were declined. This is because the thickness of the catalyst layer became rather large when the catalyst loading was further increased, greatly increasing the transfer resistance. Hence, not only the photocatalysts inside of the entire catalytic layer could not be efficiently utilized but also the mass transfer of the CO_2 and OH^- was resisted seriously. In this case, less methanol could be generated, leading to the reduction of the methanol concentration and yield. As a result, there existed an optimal catalyst loading leading to a maximum performance of the photocatalytic reduction of CO_2 with the developed microeactor.

All the above experimental results have demonstrated the superior performance of the developed optofluidic planar microreactor. Moreover, the microreactor in this work is a continuous flow reactor, which is promising in real applications. We have also compared our experimental data with the open literatures. It is found that our methanol yields with pure TiO_2 catalyst were better than some works using doping catalysts such as Rh/TiO_2 [42] and Cu/TiO_2 [16], and visible-light responsive catalysts such as NiO/$InTaO_4$ [31] and Cu/GO [43]. Although our methanol yield was lower than the Yang's data of 627 μmole/g-cat·h [40] and the Nasution's data of over 800 μmole/g-cat·h [17], Yang et al. utilized mesoporous TiO_2/SBA-15 as the catalyst, which had a relatively high specific surface area to promote the diffusion and

adsorption of reactants and Nasution et al. adopted CuO/TiO_2 catalyst which was more selective and beneficial for the methanol production. This fact proves that the optofluidic planar microreactor is one of the ideal approaches to improve the CO_2 photocatalytic reduction performance owing to enhanced mass transport and large specific surface area of the microreactor and more uniform light distribution.

4. Conclusions

The photocatalytic reduction of CO_2 shares the feature with optofluidics, i.e., the synergy of fluids, light and their interaction. In this study, therefore, an optofluidic planar microreactor was developed by incorporating optofluidics into the photocatalytic reduction of CO_2. Such incorporation enables fine flow control, high specific surface area, enhanced mass and photon transport and uniform light distribution. To evaluate the performance of the developed microreactor, the methanol concentration at the outlet was measured to estimate the methanol yield. The influences of the liquid flow rate, light intensity, NaOH concentration and catalyst loading on the photocatalytic reduction of CO_2 were investigated. Main conclusions are as follows.

(i) Increasing the liquid flow rate firstly improved and then decreased the methanol concentration because of the competition between the reactants supply and residence time and dilution effect. However, the methanol yield continuously increased as the liquid flow rate increased.

(ii) An increase in the light intensity led to the increase of the methanol concentration and yield because of more electron-hole pairs to be excited.

(iii) Increasing the NaOH concentration was able to improve both the methanol concentration and yield because of more CO_2 to be dissolved and more scavenger to be supplied for boosting the photocatalytic reaction.

(iv) The increase of the catalyst loading firstly improved the performance because of increased active surface area and more excited electron-hole pairs and then resulted in the reduction of the performance mainly because of large transfer resistances.

The experimental results have demonstrated that the optofluidic planar microreactor is able to yield pretty good performance, and it is a promising platform for the photocatalytic reduction of CO_2. It should be pointed out that although the optofluidic planar microreactors have some advantages, there exists a severe problem of the limited throughput for practical application. To boost the throughput, one of the strategies can be directed to the integration of multiple microreactors to form a module and then selection of the modules to improve the throughput based on the demand. Hence, further investigation is needed to commercialize this technology for the CO_2 photoreduction.

Acknowledgments

The authors gratefully acknowledge the financial supports of the National Natural Science Foundation of China (No. 51222603, No.51276208, No.51325602 and No.

403 51576021) and the Fundamental Research Funds for the Central Universities (No.
404 CDJZR14145502).

405

406

407 **Nomenclature**

c	methanol concentration	mmol/L
f	liquid flow rate	μL/min
m	catalyst loading	mg
M	methanol yield	μmole/g-cat·h

408

409

410 **References**

411 [1] IPCC Fourth Assessment Report: Climate Change 2007,
412 http://www.ipcc.ch/publications_and_data /ar4/syr/en/contents.html, 2007.
413 [2] National Oceanic and Atmospheric Administration,
414 http://www.esrl.noaa.gov/gmd/ccgg/trends/, 2013.
415 [3] IPCC Fifth Assessment Report: Climate Change 2013,
416 http://www.ipcc.ch/report/ar5/, 2013.
417 [4] Leung DYC, Caramanna G, Maroto-Valer M. An overview of current status of
418 carbon dioxide capture and storage technologies. Renewable and Sustainable Energy
419 Rev 2014;39:426-443.
420 [5] Centi G, Perathoner S. Opportunities and prospects in the chemical recycling of
421 carbon dioxide to fuels. Catal. Today 2009; 148: 191-205.
422 [6] Corma A, Garcia H. Photocatalytic reduction of CO_2 for fuel production:
423 Possibilities and challenges. J. Catal 2013;308:168-175.
424 [7] Adelodun AA, Kim KH, Ngila JC, Szulejko J. A review on the effect of amination
425 pretreatment for the selective separation of CO_2. Appl. Energy 2015;158:631-642.
426 [8] Ma SC, Chen GD, Zhu SJ, Yu WJ. Mass transfer of ammonia escape and CO_2
427 absorption in CO_2 capture using ammonia solution in bubbling reactor. Appl. Energy
428 2016;162:354-362.
429 [9] Al-Kalbani H, Xuan J, García S, Wang HZ. Comparative energetic assessment of
430 methanol production from CO_2: Chemical versus electrochemical process. Appl.
431 Energy 2016;165:1-13.
432 [10] Roy SC, Varghese OK, Paulose M, Grimes CA. Toward solar fuels:
433 photocatalytic conversion of carbon dioxide to hydrocarbons. ACS Nano 2010;4:
434 1259-1278.

435 [11] Das S, Daud WMAW. Photocatalytic CO_2 transformation into fuel: a review on
436 advances in photocatalyst and photoreactor. Renew Sust Energ Rev 2014;39:765–805.
437 [12] Dhakshinamoorthy A, Navalon S, Corma A, Garcia H. Photocatalytic CO_2
438 reduction by TiO_2 and related titanium containing solids. Energy Environ. Sci
439 2012;5:9217-9233.
440 [13] Wang CC, Zhang YQ, Li J, Wang P. Photocatalytic CO_2 reduction in metal–
441 organic frameworks: A mini review. J. Mol. Struct. 2015;1083:127-136.
442 [14] Tu W, Zhou Y, Zou Z. Photoconversion: Photocatalytic Conversion of CO_2 into
443 Renewable Hydrocarbon Fuels: State−of−the−Art Accomplishment, Challenges, and
444 Prospects. Adv. Mater. 2014;26:4607-4626.
445 [15] Tseng I H, Chang WC, Wu JCS. Photoreduction of CO_2 using sol–gel derived
446 titania and titania-supported copper catalysts. Appl. Catal., B 2002;37:37-48.
447 [16] Tseng IH, Wu JCS, Chou HY. Effects of sol–gel procedures on the photocatalysis
448 of Cu/TiO_2 in CO_2 photoreduction. J. Catal 2004;221:432-440.
449 [17] Nasution HW, Purnama E, Kosela S, Gunlazuardi J. Photocatalytic reduction of
450 CO_2 on copper-doped Titania catalysts prepared by improved-impregnation method.
451 Catal. Commun 2005; 6:313-319.
452 [18] Yahaya AH, Gondal MA, Hameed A. Selective laser enhanced photocatalytic
453 conversion of CO_2 into methanol. Chem. Phys. Lett 2004;400:206-212.
454 [19] Tahir M, Amin NAS. Advances in visible light responsive titanium oxide-based
455 photocatalysts for CO_2 conversion to hydrocarbon fuels. Energy Convers. Manage
456 2013;76:194-214.
457 [20] Izumi Y. Recent advances in the photocatalytic conversion of carbon dioxide to
458 fuels with water and/or hydrogen using solar energy and beyond. Coord. Chem. Rev
459 2013;257:171-186.

460 [21] Qin GH, Zhang Y, Ke XB, Sun Z, Liang M, Xue S. Photocatalytic reduction of
461 carbon dioxide to formic acid, formaldehyde, and methanol using dye-sensitized TiO_2
462 film. Appl. Catal., B 2013;129(3):599–605.
463 [22] Cheng YH, Nguyen VH, Chan HY, Wu JCS, Wang WH. Photo-enhanced
464 hydrogenation of CO_2 to mimic photosynthesis by CO co-feed in a novel twin reactor.
465 Appl. Energy2015;147:318-324.
466 [23] Habisreutinger SN, Lukas SM, Stolarczyk JK. Photocatalytic reduction of CO_2
467 on TiO_2 and other semiconductors. Angew Chem Int Edit 2013;52:7372-7408.
468 [24] Kočí K, Obalová L, Lacný Z. Photocatalytic reduction of CO_2 over TiO_2 based
469 catalysts. Chemical Papers 2008;62:1-9.
470 [25] Wang S, Hou Y, Wang X. Development of a Stable $MnCo_2O_4$ Cocatalyst for
471 Photocatalytic CO_2 Reduction with Visible Light. ACS Appl. Mat. Interfaces
472 2015;7(7) :4327-4335.
473 [26] Sun Z, Yang ZM, Liu HF, Wang HQ, Wu ZB. Visible-light CO_2 photocatalytic
474 reduction performance of ball-flower-like Bi_2WO_6 synthesized without organic
475 precursor: Effect of post-calcination and water vapor. Appl. Surf. Sci 2014;315:
476 360-367
477 [27] Pan P W, Chen YW. Photocatalytic reduction of carbon dioxide on $NiO/InTaO_4$
478 under visible light irradiation. Catal. Commun. 2007;8(10): 1546-1549.
479 [28] Tahir M, Amin NAS. Recycling of carbon dioxide to renewable fuels by
480 photocatalysis: Prospects and challenges. Renew. Sust. Energ. Rev. 2013,
481 25(5):560-579.
482 [29] Ola O, Maroto-Valer M M. Review of material design and reactor engineering on
483 TiO_2 photocatalysis for CO_2reduction. J. Photochem. Photobiol. C 2015; 24:16-42.
484 [30] Tahir M, Amin NAS. Photocatalytic CO_2 reduction with H_2O vapors using

485 montmorillonite/TiO_2 supported microchannel monolith photoreactor. Chem. Eng. J
486 2013;230:314-327.
487 [31] Liou PY, Chen SC, Wu JCS, Liu D, Mackintosh S, Maroto-valer M, Linforth R.
488 Photocatalytic CO_2 reduction using an internally illuminated monolith photoreactor.
489 Energy Environ. Sci 2011; 4:1487-1494.
490 [32] Wang N, Zhang XM, Wang Y, Yu WX, Chan HLW. Microfluidic reactors for
491 photocatalytic water purification. Lab Chip 2014;14:1074-1082.
492 [33] Ahsan SS, Gumus A, Erickson D. Redox mediated photocatalytic water-splitting
493 in optofluidic microreactors. Lab Chip 2013;13:409-414.
494 [34] Wang N, Tan F, Wan L, Wu MC, Zhang XM. Microfluidic reactors for
495 visible-light photocatalytic water purification assisted with thermolysis.
496 Biomicrofluidics 2014;8:054122.
497 [35] Li L, Wang GY, Chen R, Zhu X, Wang H, Liao Q, Yu YX. Optofluidics based
498 micro-photocatalytic fuel cell for efficient wastewater treatment and electricity
499 generation. Lab Chip 2014;14:3368-3375.
500 [36] Tahir M, Amin NAS. Photocatalytic CO_2 reduction and kinetic study over
501 In/TiO_2 nanoparticles supported microchannel monolith photoreactor. Appl. Catal., A
502 2013;467:483-496.
503 [37] Cheng X, Chen R, Zhu X, Liao Q, He XF, Li SZ, and Li L. Optofluidic
504 membrane microreactor for photocatalytic reduction of CO_2. Int. J. Hydrogen Energy
505 2016;4:2457-2465.
506 [38] He XF, Chen R, Liao Q,Wang H, Zhu X, Xu QY. IR laser assisted photothermal
507 condensation in a microchannel. Chem. Eng. Sci 2014;119:288-294.
508 [39] Lei L, Wang N, Zhang XM, Tai QD, Tsai DP, Chan HLW. Optofluidic planar
509 reactors for photocatalytic water treatment using solar energy. Biomicrofluidics

510 2010;4:043004.
511 [40] Yang HC, Lin HY, Chien YS, Wu JCS, Wu, H. H. Mesoporous TiO_2/SBA-15,
512 and Cu/TiO_2/SBA-15 composite photocatalysts for photoreduction of CO_2 to
513 methanol. Catal. Lett 2009;131:381-387.
514 [41] Li X, Faghri A. Review and advances of direct methanol fuel cells (DMFCs) part
515 I: Design, fabrication, and testing with high concentration methanol solutions. J.
516 Power Sources 2013;226:223-240.
517 [42] Ola O, Maroto-ValerM, Liu D, Mackintosh S, Lee CW, Wu JCS. Performance
518 comparison of CO_2 conversion in slurry and monolith photoreactors using Pd and
519 Rh-TiO_2 catalyst under ultraviolet irradiation. Appl. Catal., B 2012;126:172-179.
520 [43] Shown I, Hsu HC, Chang YC, Lin CH, Roy PK, Ganuly A, Wang CH, Chang JK,
521 Wu CI, Chen LC, Chen KH. Highly efficient visible light photocatalytic reduction of
522 CO_2 to hydrocarbon fuels by Cu-nanoparticle decorated graphene oxide. Nano Lett.
523 2014;14: 6097-6103.
524

Figure captions

Figure 1 (a) Design and (b) image of the optofluidic planar microreactor.

Figure 2 FE-SEM of the top-surface microstructure of the TiO_2 film.

Figure 3 The experimental system.

Figure 4 The chromatographic peak corresponding to methanol.

Figure 5 Effect of the liquid flow rate on the methanol concentration and yield. Light intensity: 8 mW/cm^2, NaOH concentration: 0.2 M, catalyst loading, 2.5 mg/cm^2.

Figure 6 Effect of the light intensity on the methanol concentration and yield. Liquid water flow rate: 50 μL/min, NaOH concentration: 0.2 M, catalyst loading: 2.5 mg/cm^2.

Figure 7 Effect of the NaOH concentration on the methanol concentration and yield. Liquid flow rate: 50 μL/min, light intensity: 8 mW/cm^2, catalyst loading: 2.5 mg/cm^2.

Figure 8 Effect of the catalyst loading on the methanol concentration and yield. Liquid flow rate: 50 μL/min, light intensity: 8 mW/cm^2.

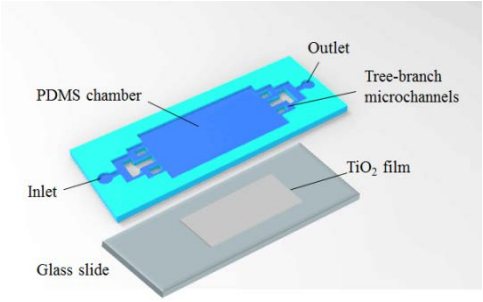

(a)

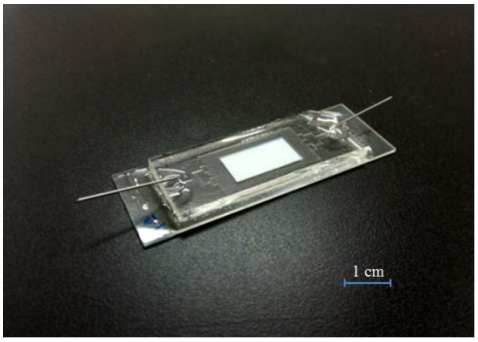

(b)

Fig. 1 (a) Design and (b) image of the optofluidic planar microreactor.

552

553

554

555

556

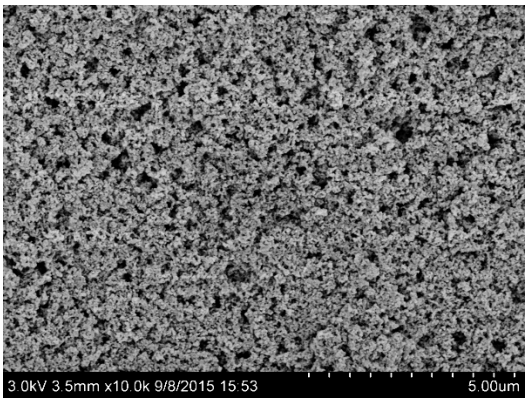

557

558

559 **Fig. 2** FE-SEM of the top-surface microstructure of the TiO_2 film.

560

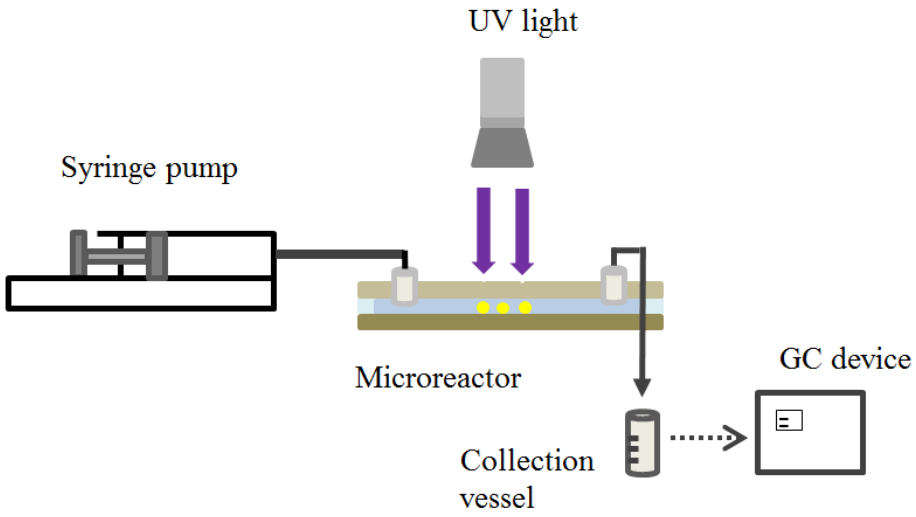

Fig. 3 The experimental system.

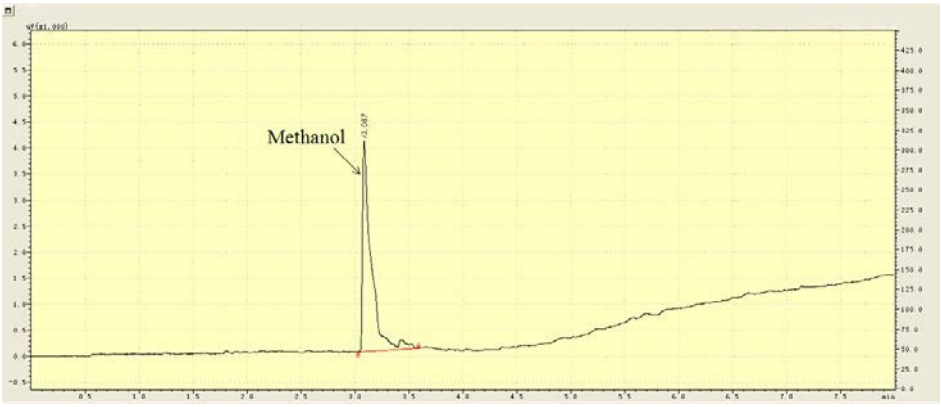

Fig. 4 The chromatographic peak corresponding to methanol.

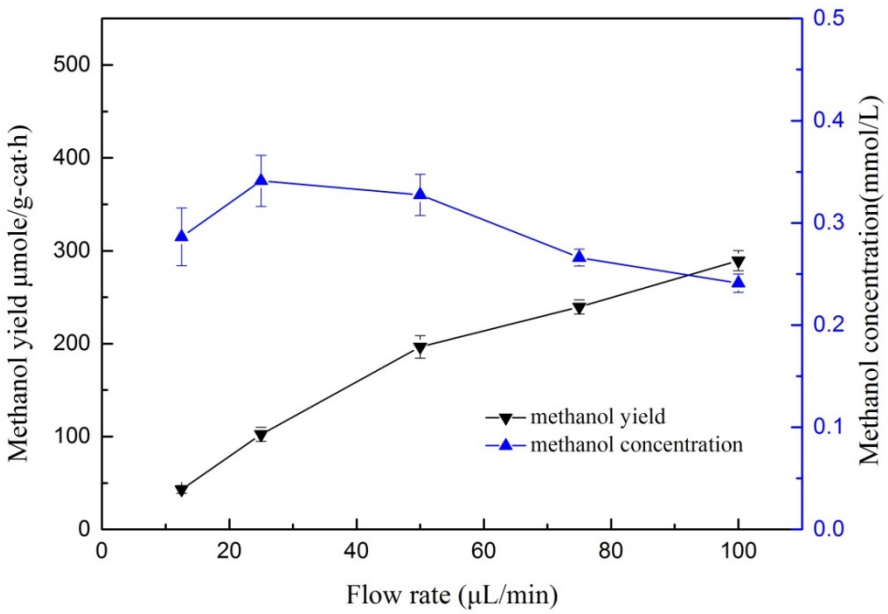

Fig. 5 Effect of the liquid flow rate on the methanol concentration and yield. Light intensity: 8 mW/cm^2, NaOH concentration: 0.2 M, catalyst loading, 2.5 mg/cm^2.

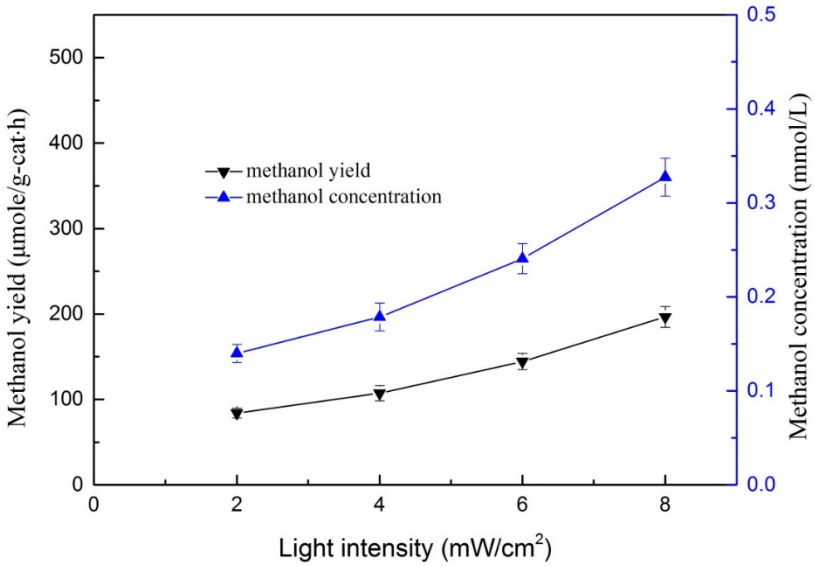

Fig. 6 Effect of the light intensity on the methanol concentration and yield. Liquid water flow rate: 50 μL/min, NaOH concentration: 0.2 M, catalyst loading: 2.5 mg/cm^2.

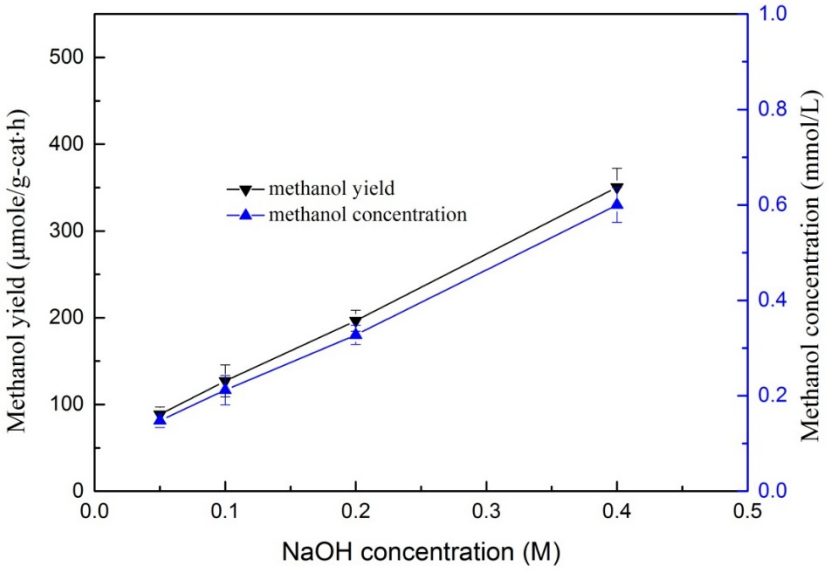

Fig. 7 Effect of the NaOH concentration on the methanol concentration and yield. Liquid flow rate: 50 μL/min, light intensity: 8 mW/cm^2, catalyst loading: 2.5 mg/cm^2.

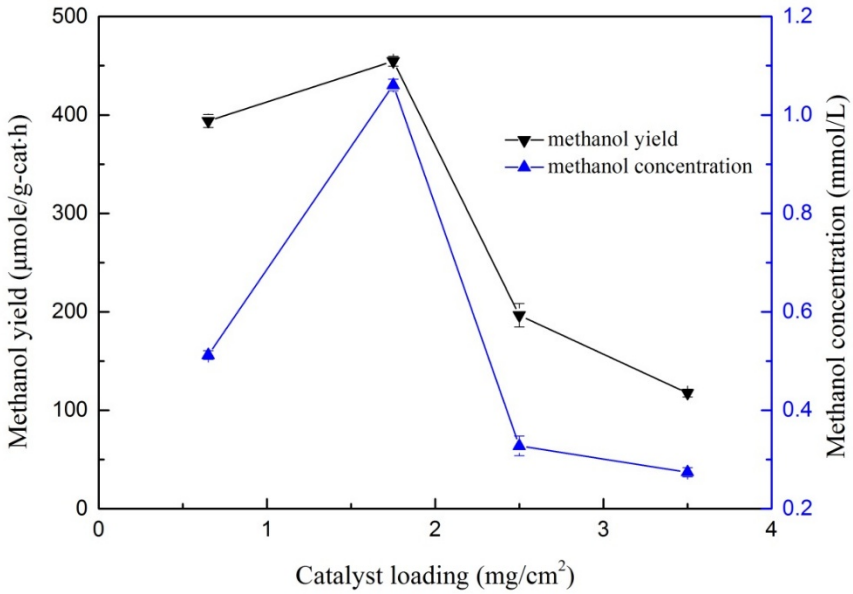

Fig. 8 Effect of the catalyst loading on the methanol concentration and yield. Liquid flow rate: 50 μL/min, light intensity: 8 mW/cm^2.